

## Microturbulence in the foot of a supercritical shock: evidence of electron cyclotron instability

L. Muschietti<sup>1</sup>, B. Lembege<sup>2</sup>

<sup>1</sup> *Space Sciences Laboratory, UCB, Berkeley, USA*

<sup>2</sup> *CETP-CNRS-UVSQ, Velizy, France*

### Introduction

A hallmark of supercritical shocks in collisionless plasmas is the existence of ions reflected off of the steep shock front. For perpendicular shock orientations, their presence shows up in the magnetic profile as a “foot”, which extends upstream of a sharp magnetic ramp. Their role is to provide the dissipation needed for shock physics. Further, from a microphysics viewpoint their existence also makes the foot region an interesting site of streaming instabilities excited by relative drifts between the beams of incoming and reflected ions, and the electrons.

By means of one-dimensional PIC simulations of perpendicular shocks with good resolution we show that an electron cyclotron microinstability can develop in the foot. The instability has a short wavelength, is electrostatic, and basically results from the coupling of electron Bernstein waves with an ion beam mode carried by the reflected ions. As such, it propagates toward upstream and has a noticeable impact on both the populations of reflected ions and the electrons, but not on the incoming ions. Our previous work [3] is herein extended to a more realistic parameter regime where ion and electron scales are widely separated and where the various electron scales, namely in decreasing order the inertia length  $\lambda_e = c/\omega_{pe}$ , the gyroradius  $\rho_e = v_{te}/\Omega_{ce}$  and the Debye length  $\lambda_d = v_{te}/\omega_{pe}$ , are also better separated.

### Simulations

The simulations are carried out in the shock frame which is at normal incidence:  $\hat{x}$  is the normal direction, while the magnetic field points in the  $\hat{z}$  direction and the motional electric field in the  $\hat{y}$  direction. The upstream plasma impinges from the left with a velocity  $V_1$ , the downstream plasma leaves to the right with a reduced velocity  $V_2$ . The Mach number  $M_A = V_1/V_A$  where  $V_A$  is the upstream Alfvén velocity, together with  $\beta_1 = \beta_e + \beta_i$ , determines the compression ratio  $r$  which controls both density and magnetic compression:  $r = V_1/V_2 = N_2/N_1 = B_2/B_1 > 1$ . We simulate a supercritical shock with  $M_A = 3.4$ ,  $\beta_e = 0.052$  and  $\beta_i = 0.034$ . A ion-to-electron mass ratio  $M/m = 400$  is used, which leads to an Alfvén velocity  $V_A/v_{te} = 0.31$  in the dimensionless units chosen. Table 1 gives detailed parameters for each species. The values of  $\lambda_e$ ,  $\rho_e$ , and  $\lambda_d$  stand in a relationship  $50|8|1.7$ , as compared to  $24|3.2|1.6$  in the previous work [3].

Table 1: Upstream parameters in normalized units

Name	Electrons	Ions
plasma frequency	$\omega_{pe} = 0.607$	$\omega_{pi} = 3.04 \cdot 10^{-2}$
gyrofrequency	$\Omega_{ce} = 0.125$	$\Omega_{ci} = 3.13 \cdot 10^{-4}$
thermal velocity	$v_{te} = 1.0$	$v_{ti} = 4.0 \cdot 10^{-2}$
drift velocity	$V_1 = 1.05$	$V_1 = 1.05$
Debye length	$v_{te}/\omega_{pe} = 1.65$	$v_{ti}/\omega_{pi} = 1.32$
inertial length	$c/\omega_{pe} = 49.5$	$c/\omega_{pi} = 990.$
gyroradius	$\rho_e = 8.0$	$\rho_i = 128.$

A look at Table 1 makes it clear that the incoming ions appear as a cold beam with a 4% spread impinging on the shock front. Under these conditions, shock front and foot undergo a cyclical evolution in a process known as self-reformation [2, 1, 4] over a period about  $\Omega_{ci}^{-1}$ . Fig. 1 displays a section of the simulation box at a time when reflected ions accumulate and the foot is building up. Shown on the left are spatial profiles of the magnetic field  $B_z$  (in blue), the electron density  $N_e$ , the current density  $J_y$  (both in black), and the electrostatic field  $E_x$  (in red). The shock front is visible at  $x \sim 90 \lambda_e$  while the foot extends upstream to  $x \sim 60 \lambda_e$ . On the right we show the associated phase-space view of the electrons and the ions. The reflection of the ions at the ramp ( $x \sim 90 \lambda_e$ ) is evident. Note the small tines that develop in the reflected ions about  $x \sim 70 \lambda_e$ . They signal the instability which is visible in the wiggly profiles of  $E_x$  and  $N_e$ .

To analyze the instability, we compute the local distribution functions of electrons and ions in the interval  $70 < x/\lambda_e < 80$  at a slightly earlier time when the instability is supposedly in its linear phase ( $t = 6750$ ). Further, we let a probe at  $x = 73 \lambda_e$  record the local values of  $B_z$ ,  $E_y$ , and  $E_x$ . Fig. 2 shows their history around time  $t \sim 7000$ . The growing, purely electrostatic instability is evident. A Fourier analysis yields a characteristic wavenumber  $k\lambda_d^* = 0.45$  and a characteristic frequency  $\omega' = 0.10 \omega_{pe}^*$ , where  $\lambda_d^*$ ,  $\omega_{pe}^*$  are the local Debye length and plasma frequency, respectively. Now, for comparing  $\omega'$  to a characteristic plasma frequency, one has to Doppler shift it into the electron bulk frame. This yields  $\omega = 0.29 \omega_{pe}^*$ . By comparison the local cyclotron frequency is  $\Omega_{ce}^* = 0.24 \omega_{pe}^*$ .

As next step, we solve numerically the dispersion relation for electron Bernstein waves interacting with an ion beam so as to examine the characteristics of a possible instability (see eq.(7) in [3] for details). Parameters are given the local values just determined. The solution is plotted in Fig. 3 for the three most unstable modes. Both wavenumber and frequency indicate that we observe the first harmonic Bernstein wave, in line with our earlier simulations [3]. Moreover,



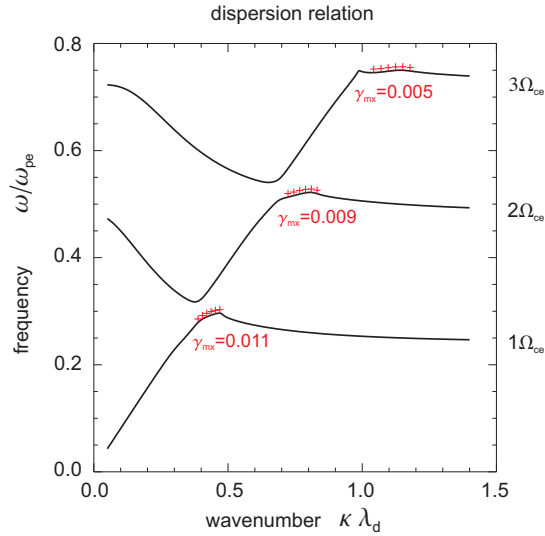


Figure 3: Electron Bernstein waves modified by the beam of reflected ions. Dispersion relation is computed with local values of plasma parameters. Ranges of growth are marked by red plusses with the maximum growth rates indicated (units of  $\omega_{pe}$ ). Note the alignment of the unstable ranges between the three harmonic branches, a signature of the coupling to the ion beam mode.

developing in the foot. Dispersion properties are analysed and are found in very good agreement with results obtained self-consistently in the simulations. The interest of such microinstability is that it occurs for a relatively low Mach number and covers small spatial scales over which the electrons develop a dynamics and break their first adiabatic invariant. In addition, it leads to some diffusion of the ion beam and hence to some local ion preheating. In [3] a theoretical model was developed to estimate the instability wavelength *a priori* from the main plasma parameters. The present instability is in line with those expectations. The ‘surprise’ deals with the wave level, which is definitely lower. An explanation might be searched in the fact that the Alfvén velocity expressed in term of electron thermal speed,  $V_A/v_{te} = 2\beta_e^{-1}m/M$ , decreases for an increasing mass ratio. Thus, relative drifts between the different populations of the foot are reduced, which means less free energy for the instabilities.

## References

- [1] Hada, T., Oonishi, M., Lembège, B., Savoini, P., J. Geophys. Res. **108**, 1233 (2003).
- [2] Lembège, B., Savoini, P., Phys. Fluids **B4**, 3533 (1992)
- [3] Muschietti, L. Lembège, B., Adv. Space Res. **37**, 483 (2006)
- [4] Scholer, M., Matsukiyo, S., Ann. Geophysicae **22**, 2345 (2004).
- [5] Shimada, N., Hoshino, M., Astrophys. J. **543**, L67 (2000)